Plasmon electron-hole resonance in epitaxial graphene

C. Tegenkamp[1], H. Pfnür[1], T. Langer[1,2], J. Baringhaus[1], and H. W. Schumacher[2]

[1] *Institut für Festkörperphysik, Leibniz Universität Hannover, Appelstrasse 2, D-30167 Hannover, Germany*

[2] *Physikalisch-Technische Bundesanstalt, Bundesallee 100, D-38116 Braunschweig, Germany*

(Dated: August 6, 2010)

Abstract

The quasiparticle dynamics of the sheet plasmons in epitaxially grown graphene layers on SiC(0001) have been studied systematically as a function of temperature, intrinsic defects, influence of multilayers and carrier density. The opening of the inter-band loss channel appears as a characteristic upward shift in the plasmon dispersion and a dip in the width of the loss peak, which is explained as a resonance effect in the formation of electron-hole pairs. Despite the existence of strong electronic correlations, the plasmon dispersion can be quantitatively described within the framework of a nearly free electron gas.

PACS numbers: 81.05.ue, 79.20.Uv, 73.20.Mf

Graphene, as a two-dimensional (2d) lattice of sp^2–hybridized carbon atoms, proves to be a model system to study fundamental questions regarding electronic correlations, collective phenomena, many-body interactions, dynamical processes and their interrelations [1–3]. Single layers can be synthesized by different techniques, e.g. exfolation of graphite or decomposition of hydrocarbons on transition metal surfaces [4, 5]. Well orientated graphene layers on insulating substrates can be grown on SiC substrates by sublimation of Si. While the morphology, the interface, the electronic structure, and even transport properties have been studied extensively in the past [6–10], plasmons in graphene have attracted notice only recently [11–13]. As we will show, for studies of this prototype of an excited collective state in 2d, graphene is indeed a perfect model system.

Although plasmons are used in nano-scaled systems, e.g, for opto-electrical conversion and resonant energy transfer processes [14], the prospects of plasmons of 2d films or even of atomic wires are still at its beginning [15, 16]. The comparatively flat dispersion in these systems provides ultrashort plasmon wavelengths. Thus, confinement on the nanometer scale becomes feasible, but strong damping of plasmon excitations and their sensitivity to defects on the atomic scale are challenges to cope with. Therefore, these studies require geometrically perfect and at the same time electronically flexible materials, such as graphene.

On the other hand, the present knowledge on 1d and 2d sheet plasmons is quite limited and, in particular, the influence of defects and the interaction with other quasi-particles is barely understood. It is clear that plasmon damping becomes dominant once the plasmon dispersion curve intersects the single particle band leading to Landau damping by single particle intra-band excitations (SPE_{intra}) as seen, e.g., in Ag/Si(111) [17, 18]. Outside the Landau regime, this mechanism is still effective, but cannot be described without explicit considerations of correlations [19–21] or momentum transfer processes [12]. Energetically low lying valence band states are considered only in terms of a polarizable background causing a quasi-linear dispersion at long wavelengths [15]. However, couplings to other particles are neither included in random phase based descriptions [20], nor were signatures of resonant coupling seen so far in experiments. Only for hybrid systems, where plasmons interact with molecular orbitals or excitonic states [22], a resonant coupling was recently reported.

In this Letter the sheet plasmon dispersion of graphene and the coupling to various decay channels is analyzed in detail by angle resolved high resolution electron energy loss spectroscopy (EELS). As we will show, once inter-band transitions are allowed by energy

and momentum conservation (SPE_{inter}), resonant coupling of this new decay channel leads to pronounced de-tuning of the plasmon frequency around Fermi energy and to an enhanced damping. The relevance of a similar type of quasiparticle dynamics in graphene, namely resonant coupling between plasmon and hole, called plasmaron, during photoemission was recently observed by Bostwick et.al. [3, 23]. It corresponds to a complementary process to that studied here, and demonstrates the importance of resonant couplings for the plasmon decay in graphene. Thus, our findings broaden the standard picture for plasmon excitations and damping mechanisms.

The growth of graphene and the measurements were performed under ultra high vacuum (UHV) condition. As substrate, Si-terminated 6H-SiC(0001) samples (n-doped, $\approx 10^{18} cm^{-3}$ from SiCrystal AG) were used and graphene was grown by sublimation of Si while annealing the SiC substrate to approximately 1500 K. Further details can be found in Refs. 9 and 12. The plasmons were measured by using a combination of high resolution electron loss spectrometer (EELS) as electron source and detector with a low energy electron diffraction system (LEED) providing simultaneously high energy and momentum ($k_{||}$) resolution [24]. Typical operating parameters were 25 meV energy resolution at a $k_{||}$ resolution of 1.3×10^{-2} Å^{-1}.

A sequence of EEL–spectra of a monolayer (ML) of graphene taken at different $k_{\|}$ values along the Γ–K direction is shown in Fig. 1. The broad loss peak can unambiguously be attributed to the sheet plasmon in graphene [11, 12]. A detailed analysis of the loss peaks (see Fig. 1 and Ref. [12]) reveals that the loss spectra can be decomposed into the main plasmon loss, two low energy phonon losses at 70 meV and 150 meV without significant dispersion, and small contributions from higher excitations, e.g, multipole plasmons. Already from Fig. 1a) it is obvious that the plasmon losses reveal two main characteristics: the halfwidth of the loss, already large at low $k_{\|}$, suddenly increases strongly around 0.1 Å^{-1} (cf. with Fig. 4). Secondly, also the peak position shifts more strongly in this range of momentum. Both features are directly linked to the opening of a new decay channel by inter-band e-h excitations, as we will show.

For this purpose, we first discuss the plasmon dispersion, shown in Fig. 2, revealing a $\sqrt{k_{\|}}$ dependence at small $k_{\|}$. It rises almost linearly up to $k_F = 0.07 \pm 0.01$ Å^{-1}, but then increases strongly again at higher $k_{\|}$ values, very much in contrast to other known plasmon dispersions in 2d systems [17, 25]. This dip in the plasmon dispersion is an intrinsic property of pristine

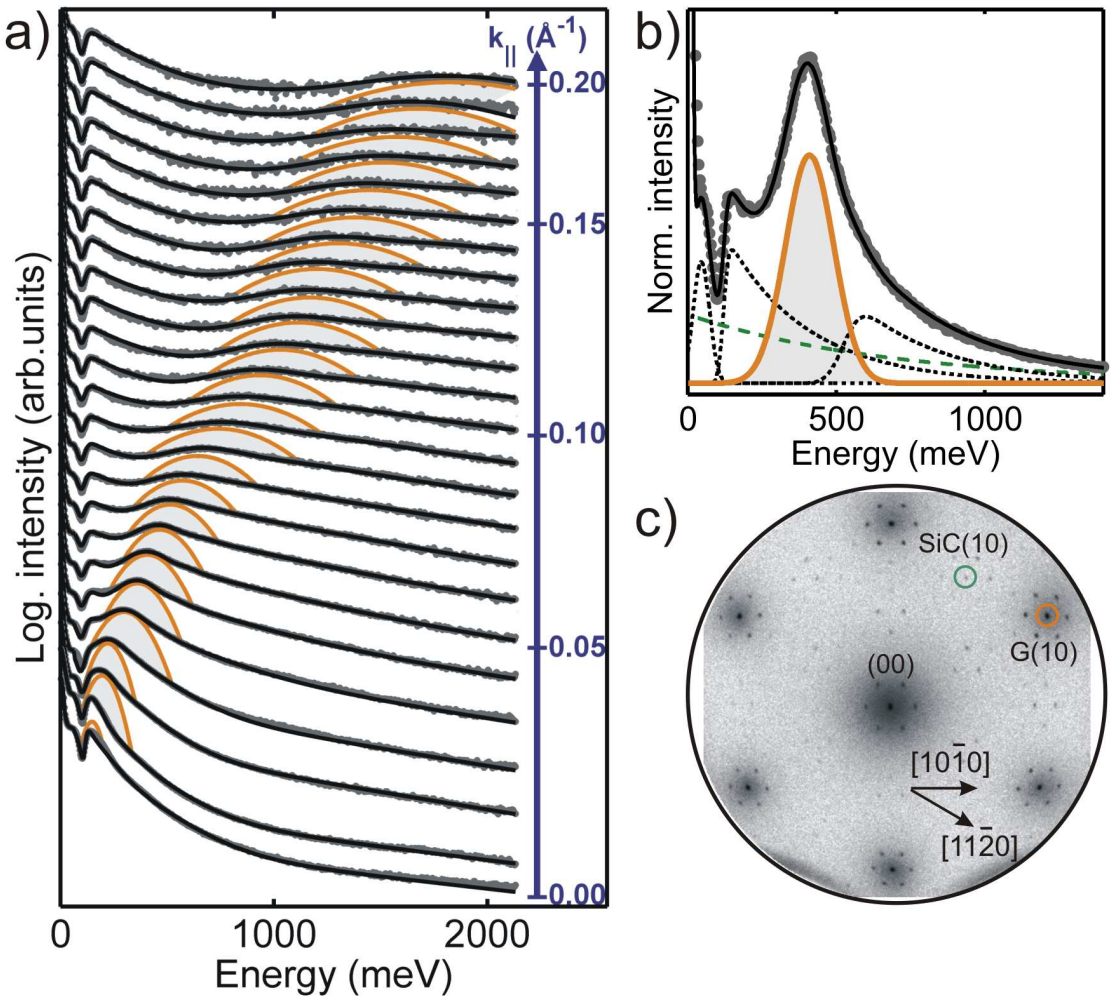

FIG. 1. (color online) a) Loss spectra (semi-log scale) for 1 ML graphene grown on H–etched SiC(0001) as a function of momentum transfer, $k_{\|}$. Primary electron energy 20 eV. Only the contribution of the 2d sheet plasmon to the loss spectrum is highlighted. b) Details of the fitting model, shown exemplarily for $k = 0.05$ $\mathring{A}^{-1}$, containing, apart from the main plasmon peak (solid line (orange)), a Drude tail (dashed (green)), phonon- and multiplasmon losses (dotted lines). For details of the fitting procedure see Ref. [12]. c) LEED pattern of 1 ML of graphene grown on SiC(0001) (E=140eV).

graphene, and does not depend on defect concentration, coupling to graphene multilayers or on temperature. Therefore, as seen from the coincidence of the dispersions measured at 80 K and at 300 K (Fig. 2), an increase of the carrier concentration by thermal activation can be ruled out as well as the coupling to high-frequency phonons. Although defects, e.g., atomic steps, influence sensitively the lifetime of the plasmons, particularly outside

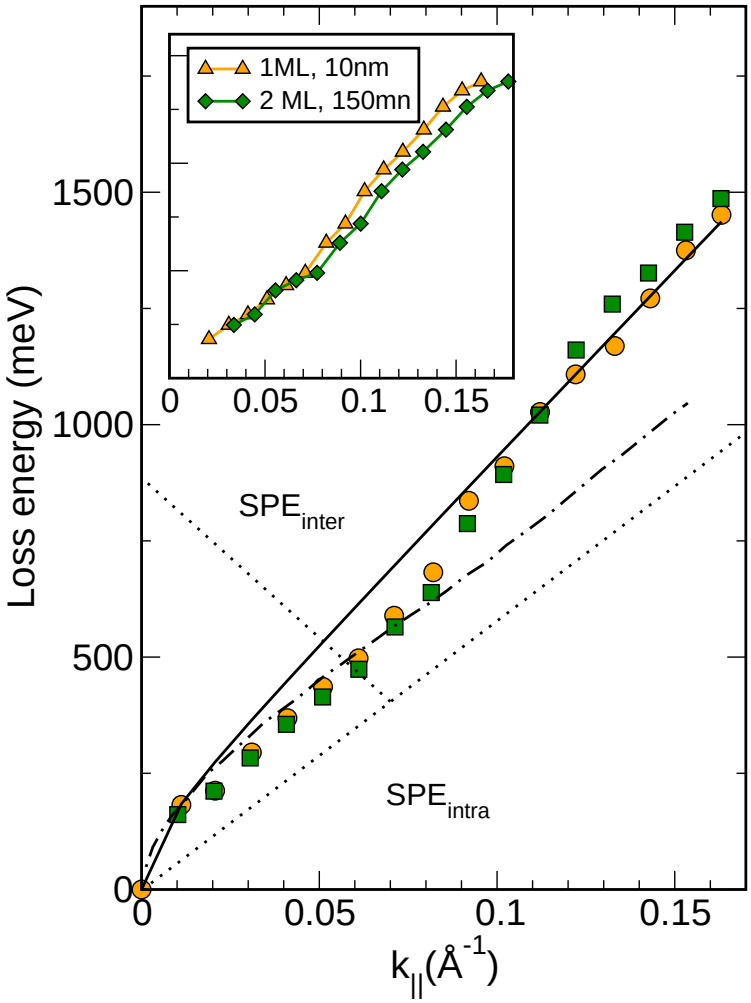

FIG. 2. (color online) Plasmon dispersion for 1 ML graphene layer (average terrace length 150 nm) grown on H–etched samples, measured at 300 K (◯) and 80 K(□). Fitted theoretical curves: nearly free electron gas ($N = 1 \times 10^{13}$cm^{-2}, 0.06 m$_e$, [29]) and with dynamical screening [20] (dashed-dotted). Dotted lines: Boundaries for intra- and inter-band SPEs derived from the graphene band structure. Inset: Independence of dispersion on step density (examples shown with terrace widths of 10nm and 150 nm) and on interaction to multilayers.

the Landau damping regime [12], the characteristics of dispersion is again unaffected, as exemplarily shown in the inset of Fig. 2. Even in presence of multilayers the dip is visible and unshifted. Only for large k–values a small redshift due to the high polarizability of the graphene layer underneath is found, which is consistent with Ref.13. The position of the dip in the dispersion does neither coincide with step periodicities nor with potential modulations caused by the superlattice of the bufferlayer underneath [26]. Hence, so-called

zone boundary collective state effects [27], as seen, e.g., in Al films [28], are not crucial in graphene. Since the filling factors are comparably low, also intervalley scattering between Dirac cones can be excluded [21]. The dip position, however, is very close to the Fermi wave vector at the given doping concentration ($E_F \approx 400meV$).

Interestingly, existing theoretical models describe only sections of this dispersion. E.g., the nearly free electron gas model (NFEG) with inclusion of first order non–local field effects, as derived by Stern [29], describes the experimental data well in the limit of large momentum transfer (k > 0.1 Å^{-1}) assuming an electron density of $N = 1 \times 10^{13} 1/cm^2$ and an effective mass of $m^* = 0.06 \pm 0.01\ m_e$ (solid line in Fig. 2). These values are close to those deduced from photoemission [6]. Inclusion of dynamic screening for both electrons and holes (dashed–dotted line, [20]) shifts the dispersion to lower values and now yields a perfect match to experiment for small $k_\parallel$ up to 0.09 Å^{-1}, but underestimates the plasmon energies in the SPE_{inter} regime. Although e-h excitations are included in these RPA descriptions, the NFEG models do not contain effects like resonant energy transfer with corresponding k-dependent changes of lifetimes. As we will show below, only the inclusion of resonant energy transfer at E_F due to opening of the inter-band e-h excitations channel allows a quantitative fit of the measured dispersion curve, now even within an extended NFEG model.

In order to observe such resonance effects between excited states, a short, but still sufficiently high lifetime τ_{e-h} at resonance is necessary in order to discriminate both types as separate excitations. As sketched in Fig. 3b) the finite value of E_F above the Dirac point in pristine graphene enables inter-band transitions at finite k-values, which are shown as vertical transitions between shifted conduction and valence band states [30]. Indeed, we can describe the whole dispersion curve in every detail (see Fig. 3a) from the loss function ($Im(-1/\epsilon)$), using simply the Drude model of the dielectric function $\epsilon = 1 - \omega_p^2/\omega(\omega + i\gamma)$, and the NFEG model of Stern assuming a resonance by opening the SPE_{inter} channel. This results in a momentum-dependent dissipation $\gamma(k)$ for the plasmons. The effective damping $\gamma(k)$ is composed of a non–resonant term $\gamma_{non-res}$, which takes into account intra-band transitions and structural imperfections, and a resonant part γ_{res}. Fig. 3c) shows the best fit result for γ. While $\gamma_{non-res}$ increases linearly with momentum [12], γ_{res} has a pronounced maximum around k_F, as expected. The asymmetry in the damping curve demonstrates further that intraband transitions at low energies contribute to the dynamic loss channel as well. This pronounced damping is clearly seen in the experiment (Fig. 3d), although the increase of

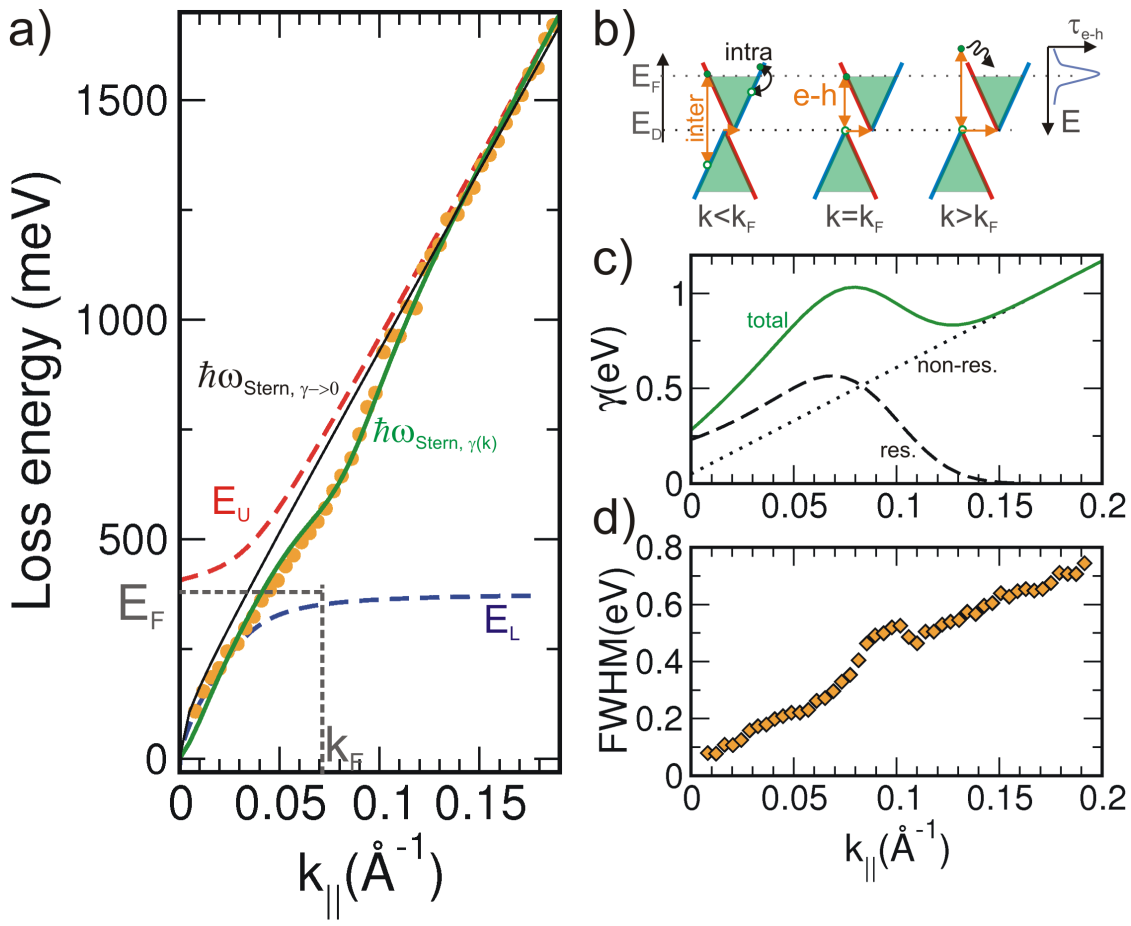

FIG. 3. (color online) a) Fits of the plasmon dispersion with the NFEG model including damping ($\hbar\omega_{Stern,\gamma(k)}$, thick(green) line) and resonant plasmon electron-hole coupling (E_U and E_L, coupling constant $2\Delta = 100\ meV$). For $\Delta = 0$ or damping constant $\gamma(k) \to 0$ the upper line ($\hbar\omega_{Stern,\gamma\to 0}$) is obtained. b) Band diagram of pristine epitaxial graphene at finite k–values demonstrating intra-band inter-band e-h pair formation at finite $k_{||}$ values. c) Effective damping $\gamma(k)$ and the decomposition into a resonant (res.) and non-resonant (non-res.) part. d) The FWHM of the plasmon loss is in qualitative agreement with $\gamma(k)$, shown in c). For details, see text.

FWHM is smaller than calculated. Finite k-resolution and the simultaneous excitations of, e.g, phonons, not considered here, may be possible reasons. Nevertheless, the resonant broadening is even seen in much broader spectra, e.g. in presence of F4-TCNQ molecules acting as defect scatterers.

This purely phenomenological description of the dip can be rationalized by a simple two-oscillator model representing plasmon and e-h-pair formation by inter-band transitions put

on-top of the non-resonant decay mechanisms. It yields a description fully consistent with the first approach. In order to see this de-tuning effect in the dispersion, the lifetimes, τ, of both oscillators need to be of same order at k_F . If further the interaction strength $2\Delta \gg \hbar/\tau$, polaritons are expected in this regime of strong coupling. The upper and lower polariton states are given by $E_{U,L}(k) = 1/2(E_{pl}(k) + E_0) \pm 1/2\sqrt{(2\Delta)^2 + (E_{pl}(k) - E_0)^2}$, where E_{pl} and E_0 are the non–interacting plasmon mode and exciton energy, respectively [31, 32]. Here we set the sheet plasmon energy $\hbar\omega_{Stern}$ for E_{pl} and the Fermi energy E_F for E_0, which is the lowest energy of interband e-h pair formation without additional momentum. 2Δ measures the interaction between the quasi-particles. The best fit yields an interaction energy of only 100 meV, in qualitative agreement with Ref. [3]. Consistent with the strongly enhanced damping determined from the fits described above, the observation of separate Rabi split states is suppressed, and only the continuous transition from the lower (E_L) to the upper branch (E_U) can be observed. In fact, also this model fits the data quantitatively with values of damping close to those determined above. Formally, this model of plasmon electron-hole interaction is closely related to interacting plasmons located in spatially separated graphene layers [19], which shows similar effects in the dispersion. However, since smooth single graphene sheets were used here, we conclude that the coupling to e-h oscillators is the dominant process.

Finally we show that the position of the dip in k-space is only influenced by the chemical potential rather than by structural parameters. For this purpose, we adsorbed a small amount of F4-TCNQ [33], which reduces the carrier density and hence shifts E_F downwards. Fig. 4 shows the dispersion after adsorption of approximately 0.01 ML at 300 K. As expected, the dip shifts to lower $k_{\|}$-values ($\approx$ 0.03 Å^{-1}). This shift is also seen in the resonance of the FWHM. Since the added molecules act as scattering centers, the loss structure is further broadened so that the exact determination of k_F from the FWHM is more difficult. Remarkably, the average slope of the dispersion remains unchanged, although the electron density at E_F is reduced to 3×10^{12}cm^{-2} due to adsorption of F4-TCNQ, which may have two possible reasons: The effective mass may be reduced by approximately the same factor when reducing the filling of the bands above the Dirac point, leaving N/m approximately constant. Secondly, the coupling of the plasmon mode with the loss channels, as evident from the large FWHM, leads to an effective integration over the electron density around E_F with a width proportional to the measured FWHM of the plasmon mode. Both the

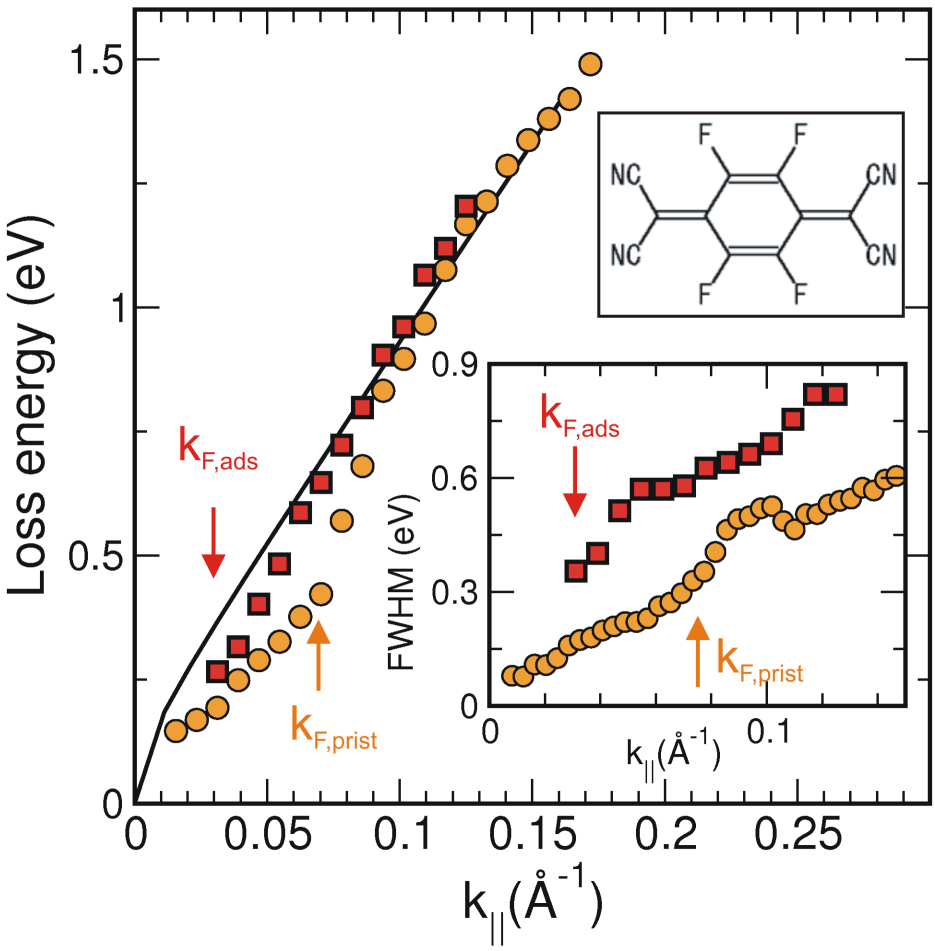

FIG. 4. (color online) Graphene plasmon dispersion before (◯) and after F4-TCNQ doping (□). Inset: corresponding changes of k-dependent FWHM. Upper inset: stereographic model of F4-TCNQ. Solid line: Fit with the NFEG model without resonant damping.

dynamics of the single and the collective excitation modes are extremely short and on the same time scale, which results in mixing of collective and single particle excitations.

In summary, the detailed analysis of plasmon excitations and their decay mechanisms, using graphene as a 2d model system, yields ultra-short dynamics with life times of the order of $\tau \approx 10^{-14}$s. Both e-h pair excitations by intra- and inter-band transitions contribute significantly to the decay of plasmons. When the latter channel is opened at finite $k_{\|}$, coupling between plasmon and e-h pair excitations is resonantly enhanced. As a consequence, characteristic modifications of the plasmon dispersion and effective integration over the density states at E_F responsible for plasmon formation were found, thus widening the standard picture for plasmon excitations.

We thank E.H. Hwang and S. Das Sarma for calculating the plasmon dispersion of graphene on the SiC dielectric (Fig. 2).

[1] K.S. Novoselov et.al., Science **306**, 666 (2004).

[2] A.K. Geim and K.S. Novoselov, Nat. Mater. **6**, 183 (2007).

[3] A. Bostwick, et.al., Science **328**, 999 (2010).

[4] J. Coraux, A.T. N'Diaye, C. Busse, and T. Michely, Nano Letters **8**, 565 (2008).

[5] P.W. Sutter, J.I. Flege, and E.A. Sutter, Nature Materials **7**, 406 (2008).

[6] T. Ohta, A. Bostwick, Th. Seyller, K. Horn, and E. Rotenberg, Science **313**, 951 (2006).

[7] C. Riedl, U. Starke, J. Bernhardt, M. Franke, K. Heinz, Phys. Rev. B **76**, 245406 (2007).

[8] K. V. Emtsev, F. Speck, Th. Seyller, L. Ley, J. D. Riley, Phys. Rev. B **77**, 155303 (2008).

[9] T. Langer, H.W. Schumacher, H. Pfnür, C. Tegenkamp, Appl. Phys. Lett. **94**, 112106 (2009).

[10] J. Haas, W.A. de Heer, and E.H. Conrad, J. Phys.: Condens. Matter **20**, 323202 (2008).

[11] Yu Liu, R.F. Willis, K.V. Emstev, Th. Seyller, Phys. Rev. B **78**, 201403(R) (2008).

[12] T. Langer, J. Baringhaus, H. Pfnür, H.W. Schumacher, C. Tegenkamp, New J. Phys. **12**, 033017 (2010).

[13] Y. Liu, R.F. Willis, Phys. Rev. B **81**, 081406(R) (2010).

[14] H.A. Atwater, A. Polman, Nature Mat. **9**, 205 (2010).

[15] B. Diaconescu, et.al. Nature **448**, 57 (2007).

[16] E.P. Rugeramigabo, et.al., Phys. Rev. B **81**, 165407 (2010).

[17] T. Nagao, T. Hildebrandt, M. Henzler, S. Hasegawa, Phys. Rev. Lett. **86**, 5747 (2001).

[18] T. Nagao, S. Yaginuma, T. Inaoka, T. Sakurai, D. Jeon, J. Phys. Soc. Jap. **76**, 114714 (2007).

[19] E.H. Hwang and S. Das Sarma, Phys. Rev. B **80**, 205405 (2009).

[20] E.H. Hwang and S. Das Sarma, Phys. Rev. B **75**, 205418 (2007).

[21] A. Hill, S. A. Mikhailov, and K. Ziegler, Europhys. Lett. **87**, 27005 (2009).

[22] W. Ni, T. Ambjörnsson, S.P. Apell, H. Chen, J, Wang, Nano Letters **10**, 77 (2010).

[23] A. Bostwick, T. Ohta, T. Seyller, K. Horn, E. Rotenberg, Nature **3**, 36 (2007).

[24] H. Claus, A. Büssenschütt, M. Henzler, Rev. Sci. Instr. **4** (1992) 2195.

[25] E.P. Rugeramigabo, T. Nagao, H. Pfnür, Phys. Rev. B **78**, 155402 (2008).

[26] S. Kim, J. Ihm, H.J. Choi, Y.W. Son, Phys. Rev. Lett. **100**, 176802 (2008).

[27] E–Ni Foo and J.J. Hopfield, Phys. Rev. **173**, 635 (1968).

[28] M. Urner–Wille, J. Phys. D: Appl. Phys. **10**, 49 (1977).

[29] F. Stern Phys. Rev. Lett. **18**, 546 (1967).

[30] R.E. Palmer, J.F. Annett, R.F. Willis, Phys. Rev. Lett. **58**, 2490 (1987).

[31] J. Bellessa, C. Bonnand, J.C. Plenet, J. Mungnier, Phy. Rev. Lett. **93**, 036404 (2004).

[32] V.M. Agranovich, M. Litinskaia, D.G. Lidzey, Phys. Rev. B **67**, 085311 (2003).

[33] W. Chen, et.al., J. Am. Chem. Soc. **129**, 10419 (2007).